

PAPER • OPEN ACCESS

Mapping and understanding the vulnerability of northern peatlands to permafrost thaw at scales relevant to community adaptation planning

To cite this article: C Gibson *et al* 2021 *Environ. Res. Lett.* **16** 055022

View the [article online](#) for updates and enhancements.

ENVIRONMENTAL RESEARCH
LETTERS

LETTER

OPEN ACCESS

RECEIVED
9 October 2020REVISED
2 February 2021ACCEPTED FOR PUBLICATION
17 February 2021PUBLISHED
11 May 2021

Original content from
this work may be used
under the terms of the
[Creative Commons
Attribution 4.0 licence](#).

Any further distribution
of this work must
maintain attribution to
the author(s) and the title
of the work, journal
citation and DOI.

Mapping and understanding the vulnerability of northern
peatlands to permafrost thaw at scales relevant to community
adaptation planningC Gibson¹ , K Cottenie¹, T Gingras-Hill^{2,3}, S V Kokelj³, J L Baltzer², L Chasmer⁴ and M R Turetsky^{1,5} ¹ Integrative Biology, University of Guelph, Guelph, ON, Canada² Biology Department, Wilfrid Laurier University, Waterloo, ON, Canada³ Northwest Territories Geological Survey, Yellowknife, NT, Canada⁴ Department of Geography, University of Lethbridge, Lethbridge, AB, Canada⁵ Institute of Arctic and Alpine Research, Colorado University, Boulder, CO 80303, United States of AmericaE-mail: cgibson3@ualberta.ca

Keywords: thermokarst, permafrost thaw, community adaptation, spatial dataset

Abstract

Developing spatially explicit permafrost datasets and climate assessments at scales relevant to northern communities is increasingly important as land users and decision makers incorporate changing permafrost conditions in community and adaptation planning. This need is particularly strong within the discontinuous permafrost zone of the Northwest Territories (NWT) Canada where permafrost peatlands are undergoing rapid thaw due to a warming climate. Current data products for predicting landscapes at risk of thaw are generally built at circumpolar scales and do not lend themselves well to fine-scale regional interpretations. Here, we present a new permafrost vulnerability dataset that assesses the degree of permafrost thaw within peatlands across a 750 km latitudinal gradient in the NWT. This updated dataset provides spatially explicit estimates of where peatland thermokarst potential exists, thus making it much more suitable for local, regional or community usage. Within southern peatland complexes, we show that permafrost thaw affects up to 70% of the peatland area and that thaw is strongly mediated by both latitude and elevation, with widespread thaw occurring particularly at low elevations. At the northern end of our latitudinal gradient, peatland permafrost remains climate-protected with relatively little thaw. Collectively these results demonstrate the importance of scale in permafrost analyses and mapping if research is to support northern communities and decision makers in a changing climate. This study offers a more scale-appropriate approach to support community adaptive planning under scenarios of continued warming and widespread permafrost thaw.

1. Background

Climate change at high latitudes is causing rapid and unprecedented environmental change (ACIA 2005; Chapin 2005) as the rate of warming across the Arctic has been three or four times that of the global average in recent decades (Bekryaev *et al* 2010, Jeffries *et al* 2013, IPCC 2018). The future impacts of climate warming on communities and infrastructure is one of the most pressing issues facing the world today (IPCC 2018). A unique challenge that northern communities face in a warming climate is the widespread thawing of permafrost. It is predicted that by the mid-21st century, the area of permafrost in

the northern hemisphere will decline by 20%–35% (IPCC 2018). Given this, northern communities are increasingly asking for decision support tools that will aid in adaptation planning by assessing where and when permafrost thaw is going to occur (Melvin *et al* 2017).

Across the discontinuous permafrost zone of the Northwest Territories (NWT), thermokarst is a common permafrost-related disturbance in northern peatlands. Permafrost peatlands typically occur as complexes of areas with intact surface permafrost (often referred to as peat plateaus or palsas) interspersed with thermokarst bogs. Thermokarst refers to the subsidence and land cover change that results

from thawing of permafrost in some areas, particularly regions with high ground ice content (Kokelj and Jorgenson 2013). In the NWT, thermokarst causes the conversion of permafrost peat plateaus to permafrost-free thermokarst bogs and shallow open water wetlands (Zoltai and Tarnocai 1974). Historically, permafrost peatlands in this region underwent a cycle of degrading permafrost followed by permafrost recovery and aggradation over an approximate 500 year period (Zoltai 1993). During the degradation or thermokarst phase, the land subsides which increases saturation causing black spruce (*P. mariana*) die off and replacement by highly productive *Sphagnum* spp. mosses. Over time, surface peat accumulation would lead to drier surface soils and greater woody plant establishment, allowing permafrost to begin to form again (Zoltai 1993). However, in a warming climate (IPCC 2018) with higher-intensity disturbance regimes (Kasischke and Turetsky 2006, Wang *et al* 2015) rates of thermokarst formation are accelerating. In the NWT, rates of thermokarst formation in peatlands increased three-fold after disturbance like wildfire (Chasmer *et al* 2010, Baltzer *et al* 2014, Gibson *et al* 2018). In many peatland-rich regions, ongoing climate change has surpassed the threshold required for permafrost recovery, meaning that permafrost thaw is irreversible (Camill 2005, Jorgenson *et al* 2006, Baltzer *et al* 2014, Gibson *et al* 2018).

Broadly, thermokarst formation can cause a cascade of direct and indirect effects, and these interact with local hydrology (e.g. Quinton and Marsh 1999, Smith *et al* 2007, Wright *et al* 2009, Tank *et al* 2016, McGuire *et al* 2018) to drastically affect community infrastructure (Addison *et al* 2016, Melvin *et al* 2017), traditional land use (Andrews *et al* 2016), soil mercury concentrations (Gordon *et al* 2016), and food security (Calmels *et al* 2015). Given these widespread and diverse impacts on ecosystem processes and services, communities and land-users will increasingly need to consider changes in permafrost within their adaptation and planning efforts (Flynn *et al* 2019). To do this effectively, there has been an increased desire and demand for permafrost modeling and vulnerability data to help inform community planning and land use planning in a warming, uncertain future. To support the development of these products (modeling and vulnerability data), geospatial analyses that describes the nature and intensity of permafrost thaw and its spatial distribution are required.

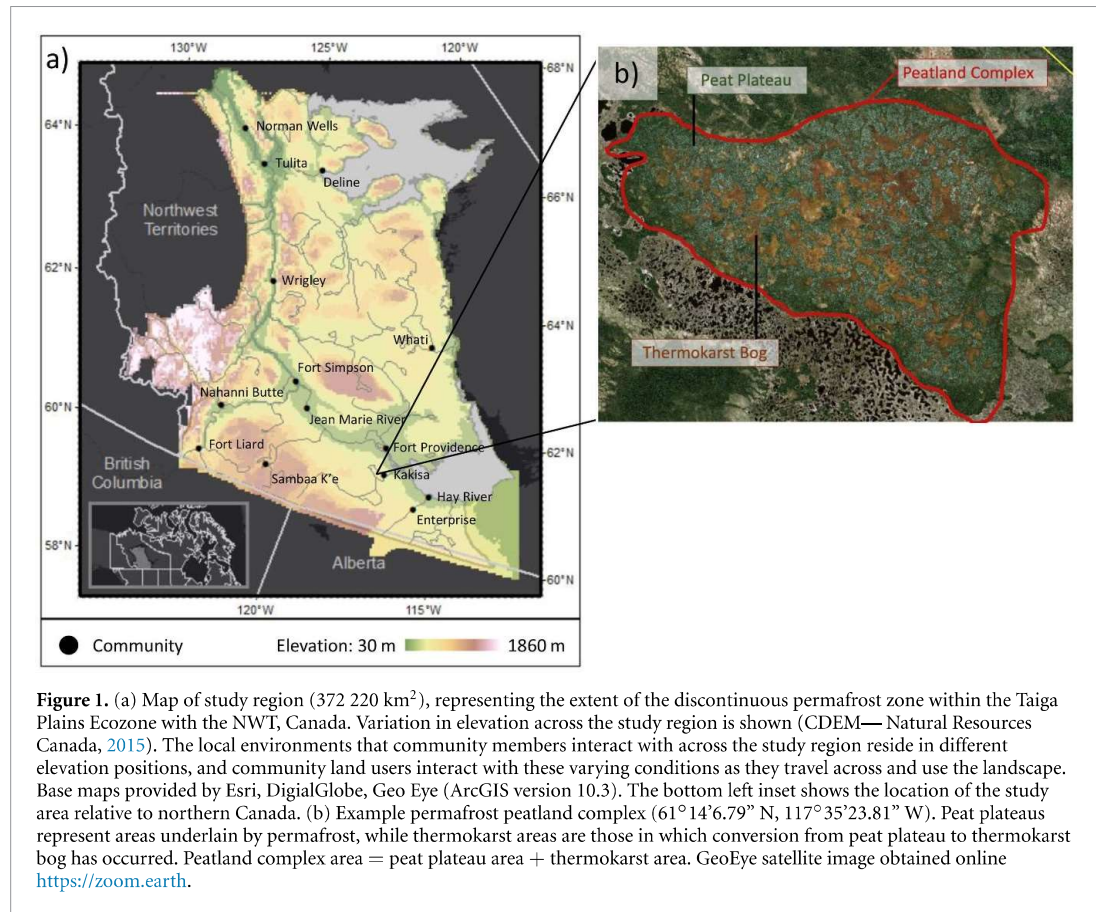
Presently, the best available data products for predicting vulnerable permafrost are either developed at circumpolar scales using modeled products (e.g. Olefeldt *et al* 2016), or are small in geographic scope, for example using fine-scale measurements for infrastructure citing projects (e.g. Flynn *et al* 2019). Some recent studies at regional scales focus on ice wedge degradation or thermokarst formation in uplands (Rudy *et al* 2017, Steedman *et al* 2017, Fraser *et al* 2018). For peatland-rich regions; however,

the Olefeldt *et al* (2016) circumpolar thermokarst maps currently offer the best description of vulnerability to thermokarst formation. As noted above, thermokarst in peatlands affects terrain stability and land use but also is relevant to conservation, wildlife, and fire management policies and planning. All of these issues require new geospatial efforts at regional to local scales.

Because permafrost is a product of climate, ground temperatures are warming in response to rising air temperatures (Biskaborn *et al* 2019). As such, mean annual air temperature is one of the most important and commonly used predictors of thaw rates (Schaefer *et al* 2014, Lawrence *et al* 2015, McGuire *et al* 2018). However, some of the most rapid thermokarst rates are occurring in cold-climates (Lewkowicz and Way 2019), a strong illustration that other factors affect the rate and extent of thermokarst formation. In the Taiga Plains region of the NWT, mean annual air temperature ranges from -1.3°C to -8.4°C . Thus, communities in this region experience very different air and ground temperatures as well as other factors such as topography and elevation (figure 1(a)) (Fick and Hijmans 2017), all of which interact to govern thaw vulnerability. The goal of this study was to work across a latitudinal gradient in the Taiga Plains region, designed to encompass some of this climatic and permafrost variability. Our geospatial analyses differentiated areas where permafrost has already thawed versus permafrost peatland areas that remain susceptible to thermokarst formation in the future. Our goals were to (a) update permafrost peatland vulnerability maps at local scales along this latitudinal gradient and compare them to the results of existing circumpolar-scale thaw products, (b) assess how the degree of thermokarst formation within permafrost peatlands varies with latitude and mean annual temperature and (c) determine the role of other topographical controls (such as elevation) on thermokarst formation and its importance for identifying vulnerable permafrost at community scales using the latitudinal gradient as a space-for-time substitution to make inferences about how thaw may progress in a warming climate. Understanding both current and future patterns of thermokarst formation in peatlands, as well as major climatic or geophysical drivers of thaw, will be important in our goal of supporting the communities whose livelihoods depend on permafrost environments.

2. Study area

This study covers an area of 372 220 km² in the south-central portion of the NWT and covers the discontinuous permafrost zone of the Taiga Plains Ecozone (figure 1(a)). Mean annual air temperature varies from -1.3°C to -8.4°C .



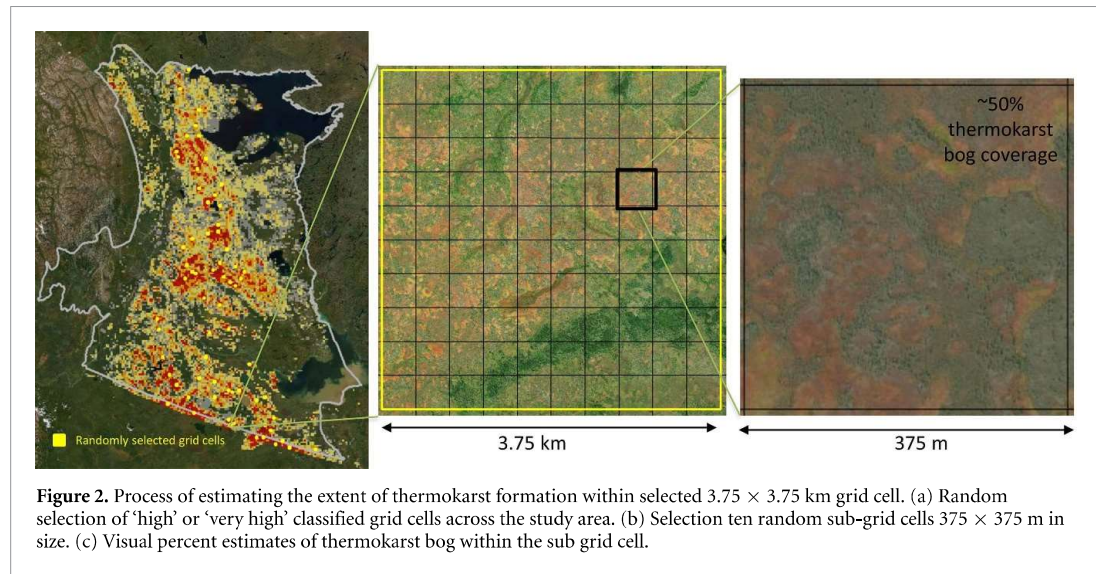
This area is characterized by a subdued relief and gently rolling plains. It is underlain with horizontal beds of sedimentary rocks consisting of limestone, shale, sandstone, and conglomerates. The imprint of glacial legacy dominates the contemporary landscape. Surficial deposits range from hummocky till, to glacially fluted terrain that has yielded vast aligned/oriented wetland and lake systems, to large lacustrine plains deposited by former glacial lakes, the largest being Glacial Lake McConnell. Post glacial incision of the Mackenzie River and its tributaries have improved drainage through the region and yielded fluvial deposits along the river valleys. However, vast low-lying areas across the region have remained poorly drained, favouring accumulation of organic materials and peatland development. As a result, this area is one of the major peatland areas of Canada and nearly 40% of the study area is peatlands (Ecosystem Classification Group (2007 rev. 2009)). Peat accumulation in this area initiated following deglaciation ~9000 years ago (Loisel et al 2014) and is strongly related to climate as well as to local moisture and drainage conditions, with peat thickness varying between 2 and 6 m. Permafrost aggradation began during the climate cooling after the Holocene thermal maximum ~5000 years ago, and became more widespread following further cooling 1200 years ago (Pelletier et al 2017).

Permafrost peatlands in this area are a mosaic of permafrost peat plateaus raised 1–2 m above surrounding permafrost-free bogs and fens. For clarity, the following definitions are used to guide the mapping and analysis as part of this study (figure 1(b)):

- **Peat plateau area:** the area where permafrost remains and elevates the surface 1–3 m above the surrounding landscape due to high ground ice content. Characterized by a relatively dry surface that supports black spruce (*Picea mariana*), evergreen shrubs such as Labrador tea (*Rhododendron groenlandicum*), and lichen and moss cover (*Cladina* spp. and *Sphagnum* spp, respectively).
- **Thermokarst area:** the permafrost-free bogs that have formed following permafrost thaw. These bogs are characterized by highly saturated soils and vegetation dominated by *Sphagnum* spp. and sedges.
- **Peatland complex area:** the entire peatland that encompasses both peat plateaus and thermokarst bog area.

2.1. Updating permafrost peatland vulnerability maps at local scales

To update permafrost peatland vulnerability maps at local scales within the discontinuous permafrost zone of the NWT, the 372 220 km² study area was



mapped using Sentinel 2 imagery (Sentinel-2A, B04 (Red), B03 (Green), B02 (Blue), 10 m, 2016 and 2017, July and August). Peatland complex area was visually mapped using a 3.75×3.75 km grid cells using the percent cover of permafrost peatland complex area per grid cell. The grid cell classes include none (0% coverage), negligible (<2%), low (3%–25%), moderate (26%–50%), high (51%–75%), and very high (76%–100%). A subset of study area (~5% of the mapped area) was assessed by two mappers in order to test the guidelines on interpretation and the accuracy of the approach. With respect to percent area estimates, overall mapper accuracy is 89%. The data was compiled and all GIS analysis was completed using ArcGIS (ESRI, 2014, version 10.2.2, Redlands, CA, USA). For complete methods and data see Gibson *et al* (2020). Given the cyclical lifecycle, and high-ice content properties of peatland permafrost (Zoltai 1993), we consider any intact permafrost peatland to be predisposed to thermokarst formation.

2.2. Assessment of the degree of thermokarst formation across a latitudinal gradient

To assess how the degree of thermokarst formation within permafrost peatland varies across the climatic gradient, we visually quantified the proportion of peatland complex area that had undergone thermokarst formation using the ESRI World Imagery map downloaded from ArcGIS.com (World Imagery (arcgis.com)). Mosaiced satellite imagery used in this interpretation were acquired during the growing season (May to September) from 2009 to 2019. All data were provided to the World Imagery archive by Maxar Inc. Data were acquired at varying pixel resolutions between 0.31 and 0.6 m collected using GeoEye-1, WorldView2, WorldView3 and Quickbird-2. Visual estimations are possible due to the distinct vegetation differences between thermokarst bogs and intact permafrost peat plateaus that are clearly discernable

on RGB (optical) high resolution satellite imagery (figure 1(b)).

To determine how the proportion of peatland complex that has thawed varied across the study region, 3.75×3.75 km grid cells with high and very high estimates of permafrost peatlands were first identified. This ensured that we were comparing similar peatlands areas across a latitudinal gradient and that differences in the amount of thaw are not being driven by other factors that are occurring at fine scales in small peatlands. Furthermore, from a community perspective, it is likely that thawing of large permafrost peatlands will have the most impact on their land use regarding travel and changes in hydrology (Quinton *et al* 2011a).

A subset of these identified cells were then randomly selected ($n = 70$, or ~5%, figure 2). Selected grid cells spanned the entirety of the study area and had high resolution ArcGIS DigitalGlobe, Geo Eye basemap (ArcGIS version 10.3) imagery available. Selected grid cells were then overlain with a 10×10 grid (creating 100 sub-grid cells with size equal to 375×375 m). Of the 100 sub grid cells, those contained within the peatland complex area were identified visually and ten random cells of those were selected to determine the degree of thermokarst formation (figure 2). In the selected sub grid cells, we visually estimated the percent of the peatland complex with thermokarst formation. Estimates were made in intervals of 10 (i.e. 0%, 10%, 20%, 30% coverage etc). The mean percent of peatland complex area that was thawed and standard deviation for each 3.75×3.75 km grid cell was calculated.

To assess how the proportion of peatland complex that has thawed varied across a climatic gradient, mean annual air temperature was estimated from WorldClim 2.1 climate model (Fick and Hijmans 2017). This dataset is a grid (resolution = 1 km^2) of average monthly temperature interpolated from

weather station data (1970–2000). Long time series of historical observations of climate and hydrology are scarce in the NWT, therefore gridded datasets have been used as alternatives to instrumental observations for climate analysis (Persaud *et al* 2020, Segal *et al* 2016). The mean annual air temperature from the WorldClim 2.1 climate model was assigned to each grid cell using the zonal statistics tool in ArcGIS. Given the high collinearity between mean annual air temperature and latitude ($R^2 = 0.95$) and the greater certainty in latitude compared to mean annual air temperature, latitude was used in all subsequent analyses.

The proportion of thawed peatland complex area was linearly regressed against latitude. The scatterplot was visually assessed for trends in thermokarst formation to make inferences about how thaw may progress in a warming climate. This data was also binned into three groups (59.9–62° N, 62–64.1° N, and 64.1–66.1° N) and statistically tested for differences in the proportion of peatland complex thawed using an ANOVA. The binned data was also statistically tested for differences in variance using a Fligner–Killeen test of homogeneity of variances for non-normally distributed data (Williams *et al* 1981).

2.3. Elevational controls on thermokarst formation

To assess the potential for elevational controls on thermokarst formation, elevation data was derived from the 0.75 arcsec (20 m) Canadian Digital Elevation Model (CDEM—Natural Resources Canada 2015). Individual CDEM tiles were mosaiced to the extent of the study area and mean elevation was assigned to each grid cell using the zonal statistic tool in ArcGIS. Visual assessments and interpretations were made to determine how elevation influenced the proportion of thermokarst formation within an individual bin and between bins. This was assessed using regression analysis with a model of the proportion of thermokarst with the main effects of latitude and elevation.

3. Results

3.1. Proportion of peatland complex that has thawed across a latitudinal gradient

The mapping of a 372 220 km² area of northwestern Canada confirmed widespread coverage of permafrost peatlands. In total, 53% of the grid cells contained permafrost peatlands (figure 3) with 16% classified as negligible, 21% low, 9% medium, 5% high, and 2% very high cover. The proportion of peatland complex already containing thaw ranged from $3 \pm 3\%$ to $77 \pm 12\%$ within the study area. The proportion of peatland complex thawed also varied along a latitudinal gradient with greater proportions of thermokarst formation in peatland complexes in the south compared to the north (figure 4(a)). The proportion

of peatland complex thawed varied between latitudinal bins (figure 4(a) inset; ANOVA, $p < 0.001$, $F = 73.89$). Additionally, there was greater variability in the proportion of peatland complex thawed in southern permafrost peatlands compared to northern ones (Fligner–Killeen test of homogeneity of variances, $p < 0.001$, figure 4(a) inset). This was also apparent from increased scatter around the regression line.

3.2. Elevational controls on thermokarst formation

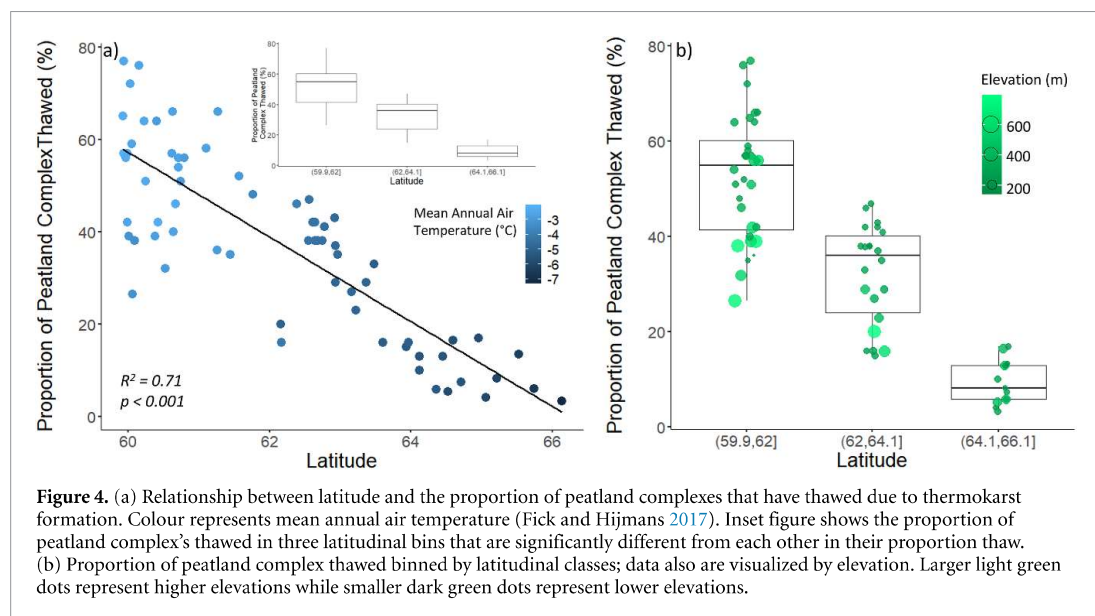
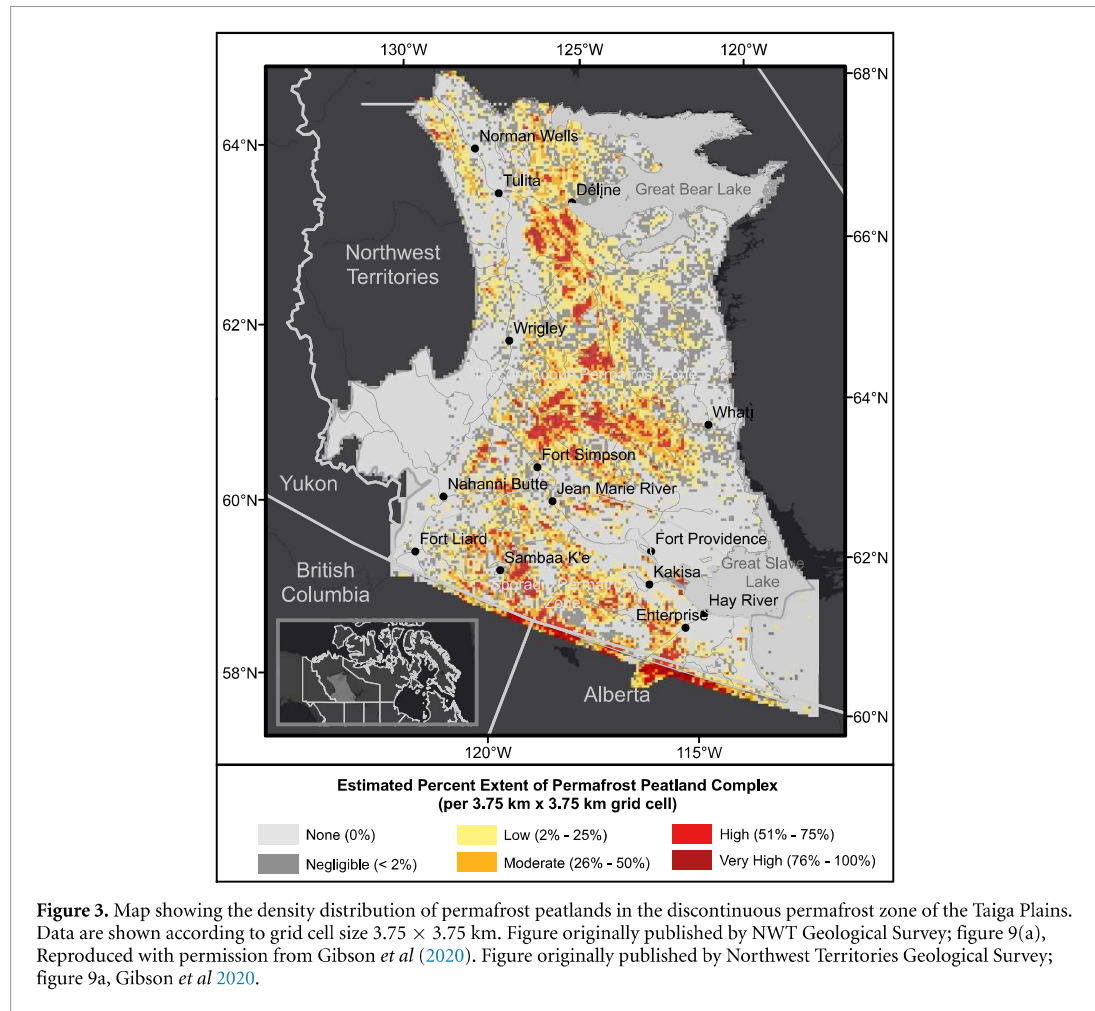
Elevation appears to govern the proportion of thermokarst formation within peatland complexes at lower latitudes (figure 4(b)). Our results suggest that latitude and elevation together improved prediction of thermokarst formation compared to latitude or mean annual air temperature alone ($p < 0.001$). Furthermore, the proportion of thermokarst formation was significantly correlated to elevation for the lower (linear model, $p = 0.004$) and mid latitude (linear model, $p = 0.006$) bins, but not for the high latitude bin (linear model, $p = 0.8$). We infer that the increased variance in the proportion of thermokarst formation at lower latitudes is being driven by this elevation effect, whereby higher elevation peatlands remain protected from increasing temperatures.

4. Discussion

4.1. New permafrost peatland thaw vulnerability map

One of the driving forces for this study was to create permafrost thaw vulnerability maps at a scale appropriate for community-use, as coarse circumpolar scale assessments can lead to feelings of eco-anxiety (Cunsolo and Ellis 2018). If thaw probability maps are coarse in scale and large areas of community territories are indicated to be ‘at high risk’ of abrupt thaw, it may contribute to feelings of hopelessness in the face of climate change (Cunsolo and Ellis 2018). The spatially explicit nature of our permafrost thaw dataset provides a more manageable perspective of risk and allow more effective identification of ‘hot spots’, and conversely also ‘cold spot’ areas that are deemed less vulnerable to landscape change in the face of warming and permafrost thaw. Additionally, the permafrost peatland and thermokarst dataset described here helps to address the subjective concept of permafrost risk (Aven and Renn 2010) in which community members are likely to carry their own risk narratives (including past experiences with permafrost thaw) and apply it to any mapping product (Flynn *et al* 2019).

Previous research used circumpolar data to quantify how much lowland organic-rich permafrost (mainly peatlands) is predisposed to thermokarst, including peatlands that may have already experienced thermokarst (Olefeldt *et al* 2016). Because of its coarse scale, Olefeldt *et al* (2016) caution against



regional or local applications of the product. Rather than relying on proxies known to be important in triggering thermokarst, such as topography or ground ice information (Olefeldt et al 2016), here we directly

quantified the area of peatland complexes and, in a subset of grid cells, the proportion of thermokarst. Because peatlands form in particular topographic and ground ice settings, our mapping product has strong

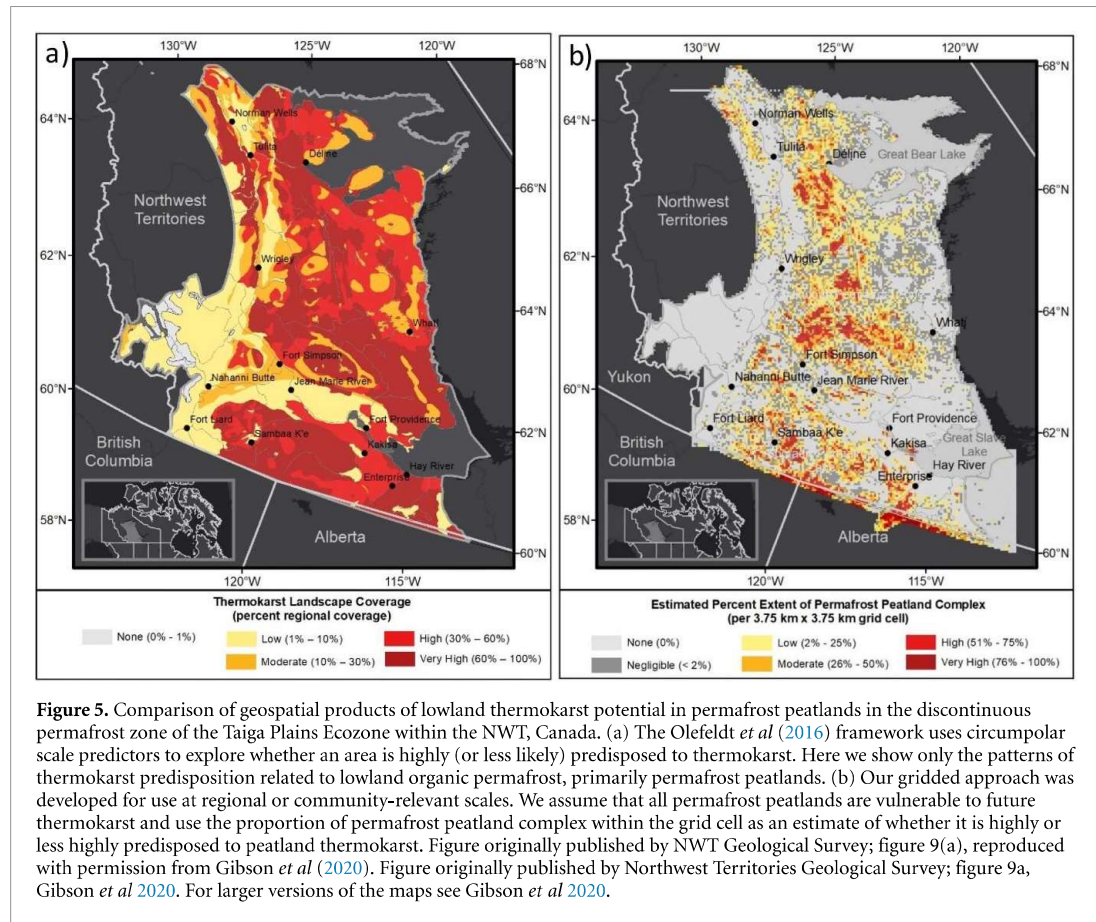


Figure 5. Comparison of geospatial products of lowland thermokarst potential in permafrost peatlands in the discontinuous permafrost zone of the Taiga Plains Ecozone within the NWT, Canada. (a) The Olefeldt *et al* (2016) framework uses circumpolar scale predictors to explore whether an area is highly (or less likely) predisposed to thermokarst. Here we show only the patterns of thermokarst predisposition related to lowland organic permafrost, primarily permafrost peatlands. (b) Our gridded approach was developed for use at regional or community-relevant scales. We assume that all permafrost peatlands are vulnerable to future thermokarst and use the proportion of permafrost peatland complex within the grid cell as an estimate of whether it is highly or less highly predisposed to peatland thermokarst. Figure originally published by NWT Geological Survey; figure 9(a), reproduced with permission from Gibson *et al* (2020). Figure originally published by Northwest Territories Geological Survey; figure 9a, Gibson *et al* 2020. For larger versions of the maps see Gibson *et al* 2020.

correlations with the input data used in Olefeldt *et al* (2016) coarser product, despite the differences between the two studies. The Olefeldt *et al* (2016) classifies ‘High’ vulnerability as 30%–60% coverage (equivalent to this study’s ‘moderate’ category) and assumes 50% of their ‘very high’ coverage to be permafrost-free given it is located in the discontinuous permafrost zone. Though these two mapping products have different approaches and vary in how the thermokarst predisposition classes were binned and classified, we were interested in comparing the two products in terms of how the area of land deemed most vulnerable to thermokarst varied (i.e. the difference in area of ‘high’ and ‘very high’ categories between the two products).

Using the circumpolar mapping approach outlined in Olefeldt *et al* (2016) applied to our study region, the proportion of total land associated with ‘high’ or ‘very high’ predisposition to lowland/peatland thermokarst was 61%. Our results indicate that only 6% of this same region has ‘high’ or ‘very high’ predisposition to peatland thermokarst based on our mapping of permafrost peatland complexes (figure 5). This reduction in the area classified as being highly predisposed to peatland thermokarst possibly is attributed to the coarse scale of input data utilized by Olefeldt *et al* (2016). The

scale of circumpolar data could be leading to an overestimation of peatland area or an overestimation of the potential for peatland thermokarst. Here we assume that all permafrost peatlands are vulnerable to thermokarst. The large differences between our results and the Olefeldt *et al* (2016) approach is likely due more to differences in classifying lowland organic-dominated terrain (Olefeldt *et al* approach) versus actual peatland area (our approach). We conclude that the Olefeldt *et al* (2016) approach is suitable for general applications that need non-spatially explicit information on thermokarst potential, while this study’s approach is appropriate for regional or fine-scale applications that require a spatially explicit understanding of where thermokarst potential areas truly are.

For purposes of community use and planning, the mapping products described in this study provide spatially explicit empirically-based estimates of permafrost peatland area and thus a more direct assessment of thermokarst potential. Given that proactive planning of infrastructure and land use based on the potential for permafrost thaw is typically more cost-effective than retrofitting (Melvin *et al* 2017), appropriately-scaled thaw vulnerability maps are critical for supporting landscape planning, cumulative effects assessments within environmental

assessments, and for environmental management through range planning. Our assumption that all permafrost peatland area is predisposed to future thermokarst is reasonable for permafrost thaw in boreal and subarctic peatlands but may not be appropriate for other types of thermokarst occurring in Arctic tundra. This means that other approaches may be required for creating community-relevant thaw vulnerability maps in regions where hillslope or lake thermokarst is likely to be a dominant type of landscape change.

We note that there are challenges in using the information from this study portrayed in figure 3 to identify future ‘hazard potential’ from thawing permafrost. A key limitation of this current dataset is that it assesses permafrost peatland complex area and does not identify the amount of thermokarst, or ‘thaw to date’ within the complex. ‘High’ classified grid cells in the north versus south can contain similar amounts of permafrost peatlands; however, peatlands located further south in our region have already experienced a significant amount of thaw (figure 4). Understanding future ‘thaw hazard’ will require a consideration of the period in which ‘hazard’ is being assessed. Southern peatlands, though they have less permafrost left to thaw (figure 4), are going to lose the remaining permafrost in much shorter timeframes than northern peatlands. Therefore, hazard assessments with shorter time frames (years to decades) would suggest higher hazard in the south, where thawing is expected to be most pronounced over this short time period. On the other hand, northern peatlands have significantly larger areas of intact permafrost remaining to thaw (figure 4), suggesting that the total magnitude of the hazard will be greater over the long term. Thus, for hazard assessments with a longer time frame (decades to next century), the potential for future thaw or thaw-hazards may be more pronounced in northern peatlands. For a more detailed description of the dataset’s limitations see Gibson *et al* (2020).

The grid-based mapping approach used in this study allowed for improved spatial resolution and continuous coverage while balancing the time required to analyse and interpret the satellite imagery. Rather than ‘mapping’ with points, lines and polygons, grid-based mapping allowed us to effectively record the locations of permafrost peatlands and identify high density area of peatlands. Grid-based mapping provides an efficient solution to the problems of mapping small landforms over large areas, by providing a consistent and standardized approach to spatial data collection (e.g. Segal *et al* 2016). The simplicity of the grid-based mapping approach makes it extremely scalable and workable for group efforts, requiring minimal user experience and producing consistent and repeatable results (Ramsdale *et al* 2017). Although the grid-based assessment cannot identify the specific locations that thaw has or is

likely to occur within the permafrost peatlands (i.e. does not identify specific thermokarst locations), what it does provide is a higher order assessment of where vulnerable areas are located. These vulnerable areas can then be assessed against important and traditional areas of communities to help direct and inform where finer scale studies and efforts should be applied (Andrews *et al* 2016). This approach is feasible because thermokarst in peatlands leads to surface changes that are easily detected. In other situations (such as active layer thickening), permafrost thaw may not be easily detected from surficial changes.

4.2. Thawed permafrost peatland areas with variation in latitude and elevational controls

The latitudinal effect on the proportion of thaw in permafrost peatland complexes illustrates the potential for continued widespread thawing across the discontinuous permafrost zone of the NWT. A near 70% difference in the proportion of thermokarst area in our study region occurs across a $\sim 3^{\circ}\text{C}$ – 4°C difference in air surface temperatures (Fick and Hijmans 2017). In response to these air temperatures, mean annual ground temperatures range from $>0^{\circ}\text{C}$ in the southern portion to -2°C in the northern portion of our study region (Smith *et al* 2010). Mean annual air temperatures in our study area are expected to rise by 3°C by 2100 (IPCC 2018). Altogether, this suggests that the ground temperatures and thaw-extent in the northern extent of the study area in the future will be similar to those currently observed in the southern extent of the study area today. Jorgenson *et al* (2020) concluded that permafrost thaw in interior Alaska, with mean air temperatures of -2.4°C , has already reached a tipping point with irreversible thaw. If this is true in the NWT, we speculate that by 2100 as much as 70% of northern permafrost peatlands will have thawed permanently within the study area.

We were surprised by the linear relationship between latitude and proportion of thermokarst. We had predicted there would be nonlinear evidence of abrupt ecological change, defined as a substantial change in ecosystem states over relatively short periods of time when compared to typical rates of change (Ratajczak *et al* 2018). Abrupt ecological changes are increasing being reported in nature due a warming climate and spans diverse ecosystems and scales (Bestelmeyer *et al* 2011, Cloern *et al* 2015, Rocha *et al* 2015, Thomson *et al* 2015, Westerling 2016). In this study, it was expected there would be a nonlinear response in the proportion of thermokarst area across the latitudinal gradient as Baltzer *et al* (2014) showed an exponential increase in the rate of thaw (i.e. percent plateau loss per year) with climate warming using a time series analysis. Although this study shows no evidence of nonlinearity in the proportion

of thermokarst area within permafrost peatlands, it could be occurring within discrete ecological areas as opposed to the larger ecological gradient we used in our space-for-time substitution. If so, additional work is needed using time series analysis to test for non-linearities within permafrost peatlands.

Our latitudinal gradient and opportunity to think about a space-for-time substitution allowed us to speculate about how northern climate-protected permafrost peatlands may be impacted by future warming. We do, however, acknowledge that our approach assumes that northern permafrost peatlands will respond to climate warming in the same way southern permafrost peatlands have. This will be complicated by complex interconnected controls on thermokarst formation including but not limited to permafrost thickness, subsurface condition, drainage and more (e.g. Quinton *et al* 2011b, Quinton and Baltzer 2013, Baltzer *et al* 2014). However, despite these cautions and caveats, space-for-time approaches are commonly used as one approach for providing insights into potential ecosystem changes associated with climate change (Dieleman *et al* 2020, Pokrovsky *et al* 2020).

One of the key challenges for predicting how and when permafrost peatlands will respond to warming is that projections often depend on accurate mean annual air temperature data. The NWT is data sparse. Mean annual air temperature data for the study region is only based on two weather reporting stations (Environment Canada 2016). While the resulting interpolation may be sufficient for large scale climate and permafrost modeling, predicting finer scale patterns and processes is difficult. If we are to support community adaptation and planning to changing permafrost conditions, we will require a better understanding of regional differences in mean annual air temperature (i.e. more long-term climate monitoring).

This study also demonstrates the importance of considering fine-scale regional differences in elevation when assessing trends in thermokarst formation. Our results show substantial variance in thaw-extent at lower latitudes. We attribute this to differences in elevation, in which higher elevation peatlands are more protected from increasing temperatures than lower elevational peatlands and are generally far better drained (figure 5). We assumed that permafrost in northern peatlands would be more climate protected than southern peatlands in our study region, but these results suggest that peatland permafrost also can be resistant to change due to high elevation. This finding, coupled with the known mean annual air temperature sparsity within the study area, introduces the need more fine-scale data. We recommend that fine-scale data collection of mean annual air temperatures and mean annual ground temperatures is prioritized in order to make more valid predictions of future permafrost thaw in and around communities.

5. Conclusion

As northern regions experience widespread permafrost thaw, northern communities need access to spatially relevant decision support tools. While several studies have quantified patterns of thermokarst sensitive terrain across a variety of scales for north-western Canada (e.g. Aylsworth *et al* 2000, Aylsworth and Kettles 2000, Kokelj *et al* 2017, Lewkowicz and Way 2019), there are few available data products for predicting the vulnerability of permafrost peatlands to thaw that bridge circumpolar (e.g. Olefeldt *et al* 2016) and very fine spatial scales (e.g. Flynn *et al* 2019). In this study we present an updated, spatially relevant dataset for predicting permafrost peatland area and thaw extent in the discontinuous permafrost zone of the NWT. This updated data product provides a more spatially explicit understanding of vulnerable permafrost peatlands and decreases the predicted area of 'high or highly vulnerable' permafrost peatlands by nearly 90%. Furthermore, we found a strong latitudinal effect on the proportion of thaw within permafrost peatland complexes, with near total loss of permafrost in the southern extent. Using this relationship in a space-for-time substitution along with climate projections for our study region, we suggest that most permafrost in peatlands across our entire latitudinal gradient across the discontinuous permafrost zone in the NWT will be permanently thawed by 2100. However, we show that thaw will be mediated by elevational differences, and that permafrost in higher elevational peatlands will be more resistant to thaw than peatlands in low elevation environments. Because northern community members interact with diverse landscapes as they access the land for hunting, gathering, and cultural activities, these differences governing the trajectory of thaw will be important to consider in regional ecosystem and infrastructure planning.

Data availability statement

Data from this study is available at: Gibson C, Morse P D, Kelly J M, Turetsky M R, Baltzer J L, Gingras-Hill T and Kokelj S V, 2020. Thermokarst Mapping Collective: Protocol for organic permafrost terrain and preliminary inventory from the Taiga Plains test area, Northwest Territories; Northwest Territories Geological Survey, NWT Open Report 2020-010, 24 pages, appendix, and digital data.

The data that support the findings of this study are openly available at the following URL/DOI: <http://webapps.nwtgeoscience.ca/WebAppsV2/Searching/ReferenceSearch.aspx?Ref=2020-010>.

Acknowledgments

We thank members of the NWT thermokarst collective for their thoughtful comments and help

in developing the mapping products. This work is a contribution to the Northwest Territories Thermokarst Mapping Collective, supported by core funding from the Climate Change Preparedness Program, Environment and Natural Resources, Government of the Northwest Territories. Additional support was provided by the National Science and Engineering Council of Canada, the Northwest Territories Cumulative Impact Monitoring Program, and CFREF Global Water Futures project Northern Water Futures, and Wilfrid Laurier University. Implementation and management of the NWT Thermokarst Collective has been possible through the Northwest Territories Geological Survey with support from GNWT-WLU partnership, NWT Centre for Geomatics, Geological Survey of Canada and Department of ENR-GNWT and several academic partners. NWT Geological Survey Contribution #0134.

ORCID iDs

C Gibson  <https://orcid.org/0000-0001-5227-5303>
M R Turetsky  <https://orcid.org/0000-0003-0155-8666>

References

- Addison P, Lautala P and Oommen T 2016 Utilizing vegetation indices as a proxy to characterize the stability of a railway embankment in a permafrost region *AIMS Geosci.* **2** 329–44
- Andrews T D, Kokelj S V, Mackay G, Buysse J, Kritsch I, Andre A and Lantz T 2016 Permafrost thaw and aboriginal cultural landscapes in the Gwich'in region, Canada *APT Bull. J. Preserv. Technol.* **47** 15–22
- Arctic Climate Impact Assessment (ACIA) 2005 Arctic Climate Impact Assessment (Cambridge: Cambridge University Press)
- Aylsworth J M, Burgess M M, Desrochers D T, Duk-Rodkin A, Robertson T and Traynor J A 2000 Surficial geology, subsurface materials, and thaw sensitivity of sediments *The Physical Environment of the Mackenzie Valley, Northwest Territories: A Base Line for the Assessment of Environmental Change* vol 547, eds L D Dyke and G R Brooks (Ottawa: Geological Survey of Canada) pp 41–7
- Aylsworth J M and Kettles I M 2000 Distribution of peatlands: in the physical environment of the Mackenzie Valley, Northwest Territories: a base line for the assessment of environmental change *Bulletin* **547** 49–55
- Baltzer J L, Veness T, Chasmer L E, Sniderhan A E and Quinton W L 2014 Forests on thawing permafrost: fragmentation, edge effects, and net forest loss *Glob. Change Biol.* **20** 824–34
- Bekryaev R V, Polyakov I V and Alexeev V A 2010 Role of polar amplification in long-term surface air temperature variations and modern arctic warming *J. Clim.* **23** 3888–906
- Bestelmeyer B T et al 2011 Analysis of abrupt transitions in ecological systems *Ecosphere* **2**
- Biskaborn B K et al 2019 Permafrost is warming at a global scale *Nat. Commun.* **10** 1–11
- Calmels F, Laurent C, Brown R, Pivot F and Ireland M 2015 How permafrost thaw may impact food security of Jean Marie River First Nation, NWT *GeoQuebec 2015 Conf. Pap.*
- Camill P 2005 Permafrost thaw accelerates in boreal peatlands during late-20th century climate warming *Clim. Change* **68** 135–52
- Chapin F S 2005 Role of land-surface changes in arctic summer warming *Science* **310**
- Chasmer L, Hopkinson C and Quinton W 2010 Quantifying errors in discontinuous permafrost plateau change from optical data, Northwest Territories, Canada: 1947–2008 *Can. J. Remote Sens.* **36** S211–23
- Cloern J E et al 2015 Human activities and climate variability drive fast-paced change across the world's estuarine-coastal ecosystems *Glob. Change Biol.* **22** 513–29
- Conover W J, Johnson M E and Johnson M M 1981 A comparative study of tests for homogeneity of variances, with applications to the outer continental shelf bidding data *Technometrics* **23** 351–61
- Cunsolo A and Ellis N R 2018 Ecological grief as a mental health response to climate change-related loss *Nat. Clim. Change* **8** 275–81
- Dieleman C M, Rogers B M, Potter S, Veraverbeke S, Johnstone J F, Laflamme J, Solvik K, Walker X J, Mack M C and Turetsky M R 2020 Wildfire combustion and carbon stocks in the southern Canadian boreal forest: Implications for a warming world *Glob Change Biol.* **26** 6062–79
- Ecosystem Classification Group 2007 (rev. 2009) Ecological Regions of the Northwest Territories – Taiga Plains (Yellowknife: Department of Environment and Natural Resources, Government of the Northwest Territories) viii + 173 pp. + folded insert map
- Environment Canada 2016 Homogenized Surface Air Temperature (AHCCD) 2016 (<https://open.canada.ca/data/en/dataset/fc09beda-744f-48df-ab7c-0949152e961f>)
- Fick S E and Hijmans R J 2017 WorldClim 2: new 1-km spatial resolution climate surfaces for global land areas *Int. J. Climatol.* **37** 4302–15
- Flynn M, Ford J D, Labbe J, Schrott L and Tagalik S 2019 Evaluating the effectiveness of hazard mapping as climate change adaptation for community planning in degrading permafrost terrain *Sustain. Sci.* **14** 1041–56
- Fraser R H, Kokelj S V, Lantz T C, McFarlane-winchester M, Olthof I and Lacelle D 2018 Climate sensitivity of high arctic permafrost terrain demonstrated by widespread ice-wedge thermokarst on Banks Island *Remote Sens.* **10**
- Gibson C M, Chasmer L E, Thompson D K, Quinton W L, Flannigan M D and Olefeldt D 2018 Wildfire as a major driver of recent permafrost thaw in boreal peatlands *Nat. Commun.* **9**
- Gibson C, Morse P D, Kelly J M, Turetsky M R, Baltzer J L, Gingras-Hill T and Kokelj S V 2020 Thermokarst Mapping Collective: Protocol for organic permafrost terrain and preliminary inventory from the Taiga Plains test area, Northwest Territories (Yellowknife: Northwest Territories Geological Survey) NWT Open Report 2020-010, 24 pages, appendix, and digital data.
- Gordon J, Quinton W, Branfireun B A and Olefeldt D 2016 Mercury and methylmercury biogeochemistry in a thawing permafrost wetland complex, Northwest Territories, Canada *Hydrol. Process.* **30** 3627–38
- IPCC 2018 Summary for policymakers. Global Warming of 1.5 °C An IPCC Special Report on the impacts of global warming of 1.5 °C above pre-industrial levels and related global greenhouse gas emission pathways, in the context of strengthening the global response to the threat of climate change, sustainable development, and efforts to eradicate poverty eds Masson-Delmotte V et al (Geneva: World Meteorological Organization) p 32
- Jeffries M O, Overland J E and Perovich D K 2013 The Arctic shifts to a new normal *Physics Today* **66** 35–40
- Jorgenson M T, Douglas T A, Liljedahl A K, Roth J E, Cater T C, Davis W A, Frost G V, Miller P F and Racine C H 2020 The roles of climate extremes, ecological succession, and hydrology in repeated permafrost aggradation and degradation in fens on the Tanana Flats, Alaska *J. Geophys. Res. Biogeosci.* **125** e2020JG005824

- Jorgenson M T, Shur Y L and Pullman E R 2006 Abrupt increase in permafrost degradation in Arctic Alaska *Geophys. Res. Lett.* **33**
- Kasischke E S and Turetsky M R 2006 Recent changes in the fire regime across the North American boreal region—Spatial and temporal patterns of burning across Canada and Alaska *Geophys. Res. Lett.* **33**
- Kokelj S V and Jorgenson M T 2013 Advances in thermokarst research *Permafrost and Periglac. Process.* **24** 108–19
- Kokelj S V, Lantz T C, Tunnicliffe J, Segal R and Lacelle D 2017 Climate-driven thaw of permafrost preserved glacial landscapes, northwestern Canada *Geology* **45** 371–74
- Lawrence D M, Koven C D, Swenson S C, Riley W J and Slater A G 2015 Permafrost thaw and resulting soil moisture changes regulate projected high-latitude CO₂ and CH₄ emissions *Environ. Res. Lett.* **10** 094011
- Lewkowicz A G and Way R G 2019 Extremes of summer climate trigger thousands of thermokarst landslides in a High Arctic environment *Nat. Commun.* **10**
- Loisel J et al 2014 A database and synthesis of northern peatland soil properties and Holocene carbon and nitrogen accumulation *Holocene* **24** 1028–42
- McGuire A D 2018 Dependence of the evolution of carbon dynamics in the northern permafrost region on the trajectory of climate change *Proc Natl Acad Sci USA* **115** 3882–87
- Melvin A M et al 2017 Climate change damages to Alaska public infrastructure and the economics of proactive adaptation *Proc. Natl Acad. Sci.* **114** E122–31
- Natural Resources Canada 2015 Canadian Digital Elevation Model (https://open.canada.ca/data/en/dataset/7f245e4d-76c2-4caa-951a-45d1d2051333?activity_id=b9b143a0-447d-4a1d-9f13-8d5f4dc0fa33)
- Olefeldt D et al 2016 Circumpolar distribution and carbon storage of thermokarst landscapes *Nat. Commun.* **7** 1–11
- Pelletier N, Talbot J, Olefeldt D, Turetsky M, Blodau C, Sonnentag O and Quinton W L 2017 Influence of Holocene permafrost aggradation and thaw on the paleoecology and carbon storage of a peatland complex in northwestern Canada *Holocene* **27** 1391–405
- Persaud B D, Whitfield P H, Quinton W L and Stone L E 2020 Evaluating the suitability of three gridded-datasets and their impacts on hydrological simulation at Scotty Creek in the southern Northwest Territories, Canada *Hydrol. Process* **34** 898–913
- Pokrovsky O S, Manasypov R M, Kopysov S G, Krickov I V, Shirokova L S, Loiko S V, Lim A G, Kolesnichenko L G, Vorobyev S N and Kirpotin S N 2020 Impact of permafrost thaw and climate warming on riverine export fluxes of carbon, nutrients and metals in Western Siberia *Water* **12**
- Quinton W L and Baltzer J L 2013 Changing surface water systems in the discontinuous permafrost zone: implications for streamflow *Cold and Mountain Region Hydrological Systems Under Climate Change: Towards Improved Projections Proceedings July 2013 Gothenburg, Sweden*, A Gelfan, D Yang, Y Gusev and H Kunstmann (IAHS Publication) pp 85–92
- Quinton W L, Chasmer L E and Petrone R M 2011a Permafrost loss and a new approach to the study of subarctic ecosystems in transition *Proceedings of symposium H02 held during IUGG2011 July 2011 Melbourne, Australia*, D Yang, P Marsh and A Gelfan (IAHS Publication) pp 98–102
- Quinton W L, Hayashi M and Chasmer L E 2011b Permafrost-thaw-induced land-cover change in the Canadian subarctic: implications for water resources *Hydrol. Process.* **25** 152–8
- Quinton W L and Marsh P 1999 A conceptual framework for runoff generation in a permafrost environment *Hydrol. Process.* **13** 2563–81
- Ramsdale J D et al 2017 Grid-based mapping: a method for rapidly determining the spatial distributions of small features over very large areas *Planet. Space Sci.* **140** 49–61
- Ratajczak Z, Stephen C, Ives A, Kucharik C, Ramiadantsoa T, Stenger M, Williams J, Zhang J and Turner M 2018 Aprupt change in ecological systems: inference and diagnosis *Trends Ecol. Evol.* **33** 513–26
- Rocha J C, Peterson G D and Biggs R 2015 Regime shifts in the anthropocene: drivers, risks, and resilience *PLoS One* **10** 10–2
- Rudy A C A, Lamoureux S F, Kokelj S V, Smith I R and England J H 2017 Accelerating thermokarst transforms Ice-cored terrain triggering a downstream cascade to the ocean *Geophys. Res. Lett.* **44** 11080–7
- Schaefer K, Lantuit H, Romanovsky V E, Schuur E A G and Witt R 2014 The impact of the permafrost carbon feedback on global climate *Environ. Res. Lett.* **9** 085003
- Segal R A, Lantz T C and Kokelj S V 2016 Acceleration of thaw slump activity in glaciated landscapes of the Western Canadian Arctic *Environ. Res. Lett.* **11** 034025
- Smith L C, Sheng Y and Macdonald G M 2007 A first pan-Arctic assessment of the influence of glaciation, permafrost, topography and peatlands on northern hemisphere lake distribution *Permafrost. Periglac. Process.* **18** 201–8
- Smith S L, Romanovsky V E, Lewkowicz A G, Burn C R, Allard M, Clow G D, Yoshikawa K and Throop J 2010 Thermal state of permafrost in North America: a contribution to the international polar year *Permafrost. Periglac. Process.* **21** 117–35
- Steedman A E, Lantz T C and Kokelj S V 2017 Spatio-temporal variation in high-centre polygons and ice-wedge melt ponds, Tuktoyaktuk coastlands, Northwest Territories *Permafrost. Periglac. Process.* **28** 66–78
- Tank S E, Striegl R G, McClelland J W and Kokelj S V 2016 Multi-decadal increases in dissolved organic carbon and alkalinity flux from the Mackenzie drainage basin to the Arctic Ocean *Environ. Res. Lett.* **11** 054015
- Terje Aven and Ortwin Renn Concepts, Guidelines and Applications 2010 Risk Management and Governance 16 Risk, Governance and Society (Berlin: Springer)
- Thomson J A, Burkholder D A, Heithaus M R, Fourqurean J W, Fraser M W, Statton J and Kendrick G A 2015 Extreme temperatures, foundation species, and abrupt ecosystem change: an example from an iconic seagrass ecosystem *Glob. Change Biol.* **21** 1463–74
- Wang X, Thompson D K, Marshall G A, Tymstra C, Carr R and Flannigan M D 2015 Increasing frequency of extreme fire weather in Canada with climate change *Clim. Change* **130** 573–86
- Westerling A 2016 Increasing western US forest wildfire activity: sensitivity to changes in the timing of spring *Phil. Trans. R. Soc. B* **371**
- Wright N, Hayashi M and Quinton W L 2009 Spatial and temporal variations in active layer thawing and their implication on runoff generation in peat-covered permafrost terrain *Water Resour. Res.* **45**
- Zoltai S C 1993 Cyclic development of permafrost in the peatlands of Northwestern Canada *Arct. Alp. Res.* **25** 240–6
- Zoltai S C and Tarnocai C 1974 Perennially frozen peatlands in the western Arctic and Subarctic of Canada *Can. J. Earth Sci.* **12** 28–43